Ab Initio Modelling the Effect of Oxidation Coupled with HnO Deprotonation on Carboxylate Ligands in Mn/Ca Clusters.

ARTICLE *in* THE JOURNAL OF PHYSICAL CHEMISTRY B · MARCH 2014

Impact Factor: 3.3 · DOI: 10.1021/jp500362q · Source: PubMed

5 AUTHORS, INCLUDING:

Wooi Yee Chuah
Australian National University
2 PUBLICATIONS **1** CITATION
SEE PROFILE

Robert Stranger
Australian National University
175 PUBLICATIONS **2,496** CITATIONS
SEE PROFILE

Elmars Krausz
Australian National University
218 PUBLICATIONS **3,333** CITATIONS
SEE PROFILE

THE JOURNAL OF PHYSICAL CHEMISTRY B

Article

pubs.acs.org/JPCB

Ab Initio Modeling of the Effect of Oxidation Coupled with H_nO Deprotonation on Carboxylate Ligands in Mn/Ca Clusters

Wooi Yee Chuah, Rob Stranger,* Ron J. Pace,* Elmars Krausz,* and Terry J. Frankcombe*

Research School of Chemistry, Australian National University, ACT 0200, Australia

Supporting Information

ABSTRACT: Oxidation of some manganese complexes containing both carboxylate and water/hydroxo ligands does not result in changes to the carboxylate stretching frequencies. The water oxidizing complex of photosystem II is one motivating example. On the basis of electronic structure theory calculations, we here suggest that the deprotonation of water or hydroxo ligands minimizes changes in the vibrational frequencies of coligating carboxylates, rendering the carboxylate modes "invisible" in FTIR difference spectroscopy. This deprotonation of water/hydroxo ligands was also found to balance the redox potentials of the Mn(II)/Mn(III) and Mn(III)/Mn(IV) couples, allowing the possibility for successive manganese oxidations at a relatively constant redox potential.

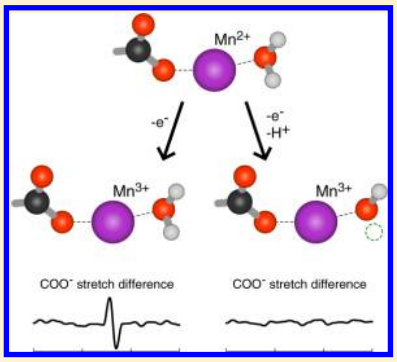

INTRODUCTION

The literature indicates that certain manganese complexes containing water and hydroxo ligands exhibit interesting behavior with respect to the effect of oxidation.[1−6] In particular, deprotonation of a ligand reduces the redox potential required to oxidize the complex, equalizes the redox potential between successive oxidation steps and suppresses vibrational frequency changes in carboxylates also ligated to the Mn center. For example, the carboxylate-bridged Mn dimer complexes studied by Eilers et al.[1] clearly deprotonate deuterated water during oxidation, but the frequencies of carboxylate stretches remain unchanged. This is in contrast to the oxidation of manganese complexes with no deprotonatable groups, which results in carboxylate stretching frequencies changing by up to 100 cm^{-1}.[7]

One important system where these properties may be relevant is photosystem II (PS II). PS II is the enzyme found within all plants, algae, and oxygenic photosynthetic bacteria that catalyzes the oxidation of two water molecules to molecular oxygen, releasing four electrons (as reducing equivalents) and four protons.[8−10] Water oxidation occurs within a metal cluster composed of four manganese ions, five oxo bridges and a calcium ion, which is known as the water oxidizing complex (WOC) or oxygen evolving complex (OEC).[11] Reaction at the WOC proceeds via four photo-induced, single electron oxidation steps through five intermediates of the WOC, called S states, S_0 to S_4. A broad range of spectroscopic methods have been used to probe the WOC, but the analysis of these results has often yielded counterintuitive or conflicting interpretations.[12]

Several crystal structures of PS II are available,[13−18] including the most recent at 1.9 Å resolution.[17,18] These PS II structures now identify all amino acid ligands to the WOC cluster and the most recent also reveal the oxo bridging between the metal ions (Figure 1).

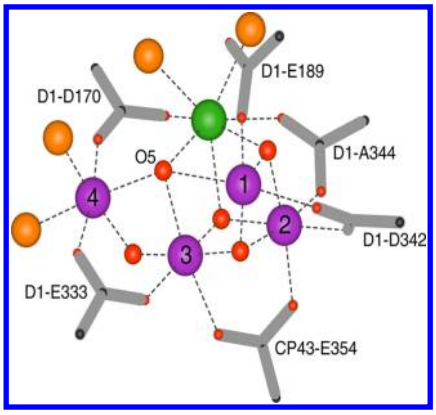

Figure 1. Ligand structure of the WOC.[17,18] Mn atoms purple, Ca atom green, amino acid side chain carboxylates as gray skeleton, O atoms red, with O atoms presumed to be water molecules orange.

FTIR turnover difference spectroscopy on functional PS II preparations, coupled with site directed mutagenesis, has been extensively applied by several groups to determine which amino acid ligands show changes in vibrational modes on specific S state advancements. Such frequency changes, particularly in carboxylate stretches (in the vicinity of 1300−1400 cm^{-1} and 1600 cm^{-1}), are expected to occur if the ligated metal undergoes oxidation. Although Mn XANES measurements

Received: January 13, 2014
Revised: March 3, 2014
Published: March 7, 2014

   dx.doi.org/10.1021/jp500362q | J. Phys. Chem. B 2014, 118, 3553−3558

(see, e.g., Dau and Haumann[19]) clearly show progressive oxidation of the Mn cluster with each S state turnover to S_3, the FTIR data have proved surprisingly opaque. FTIR signals associated with the vibrations of carboxylates not ligated to the Mn_4Ca core show that these carboxylates change vibrational frequency as the catalytic oxidation cycle progresses,[20−22] consistent with the influence of changes in the hydrogen bonding network and liberated protons and electrons.[19,23,24] Among the six carboxylates directly ligated to the Mn_4Ca core,[17,18] the stretching vibrations of the terminal carboxylates of D1-Ala344[12,25,26] and CP43-Glu354[12,27,28] change measurably through the S state cycle. Confusingly, D1-Asp170, D1-Glu189, and D1-Glu333 have been shown to not significantly change through the S state cycle,[12,29] whereas Strickler et al.[30] conclude that the evidence is also too weak to support changes to D1-Asp342. This is despite these carboxylates being ligated directly to at least one of Mn1, Mn3 or Mn4 of the WOC.

One conclusion that could be drawn from the negative results (i.e., the equivalence of wild type and mutant turnover difference spectra to within about 5 cm^{-1}) on the Mn1, Mn3, and Mn4 ligand studies is that these Mn centers do not undergo any redox change throughout the complete catalytic S cycle.[12] Such an unlikely scenario conflicts with a range of other data,[31] suggesting other factors must be influencing the FTIR turnover results. As proton loss from the WOC through the catalytic cycle is well documented,[19] the effects of coligand deprotonation is one possible explanation.

Our hypothesis is that the suppression of changes in the vibrational frequencies of carboxylate ligands by deprotonation of water/hydroxo coligands is a general feature of Mn complexes. The apparent lack of FTIR sensitivity of WOC ligated carboxylates might then be explained, although this is difficult to test in detail for a system of the complexity of the WOC. In this work we test the chemistry of this idea by investigating a set of model clusters containing carboxylate and water ligands, structurally reminiscent of components within the WOC, using ab initio electronic structure theory methods.

METHODS

Clusters containing at least one manganese atom with one formate and various water and hydroxo ligands were constructed, and the total energies of these clusters were calculated at various levels of theory using the Gaussian 09 package.[32] Frequency calculations were performed after geometry optimization. Calculations were performed at the Hartree−Fock (HF), perturbation theory (MP2), and coupled-cluster (CCSD) levels of theory, as well as using density functional theory with the M06L functional. Results listed as "HF" are from restricted open-shell Hartree−Fock (ROHF) calculations. Calculations were performed using two basis set combinations. In one set of calculations the 6-31G(d,p) basis set was used throughout. As the description of the electronic structure of the metal ions was considered to be particularly important for correctly describing the effect of changing the manganese oxidation state, in another set of calculations the 6-31G(d,p) basis set was replaced by the SDD basis set with its associated effective core potential for Mn and Ca atoms. The results presented below are for the SDD basis set on the metals, unless noted otherwise. Additional results given as Supporting Information.

Three model clusters were selected to investigate a range of carboxylate ligand bonding modes. Specifically, the three clusters exhibited unidentate Mn ligation, Mn−Mn bridging, and Mn−Ca bridging. These are labeled clusters **A**, **B**, and **C**, respectively. Water and hydroxo ligands were added consistent with the environment found in the WOC.

The clusters were assumed to have fully closed-shell ligands with the manganese center(s) in the high-spin state. To model "direct oxidation", an electron was removed from the cluster, whereas an electron and a proton would be removed for "oxidation with deprotonation". The oxidation state of the metal centers and that of ligands was assessed by examining the calculated Mulliken charges and, in particular, the Mulliken spin density. The carboxylate symmetric and asymmetric stretching normal modes were identified by inspection.

The redox potentials of the clusters were calculated as

$$E_{\mathrm{redox}} = E_{\mathrm{oxidized}} + nE_{\mathrm{H}} - E_{\mathrm{initial}} \quad (1)$$

where E_{initial}, E_{H}, and E_{oxidized} are the energies calculated for the cluster before oxidization, the hydrogen atom, and the oxidized cluster, respectively, and n is the number of protons removed (n = 0 or 1).

One may suspect the formate ligands used in this work to be a crude approximation to the amino acids ligated to the metal ion clusters found in biological systems, and that longer carbon chain carboxylate ligands may make a better model. However, exploratory calculations suggest that the results obtained using, for example, acetate ligands are similar to those presented here using formate ligands. Formate ligands have been used for their lower computational cost.

RESULTS

Geometries of clusters **A**, **B**, and **C** are shown in Figures 2−4, respectively. The geometries from optimizations at the ROHF level [with the mixed 6-31G(d,p) and SDD basis set] were used to generate these figures. The optimized geometries for the Mn(II) clusters are shown at the top, with structural changes on oxidation without and with deprotonation shown below.

The frequency shifts in the carboxylate ligand on oxidation of **A**, **B**, and **C** are given in Tables 1−3, respectively. A missing entry in these tables indicates that the corresponding calculation could not be converged. This occurred exclusively for MP2 and CCSD calculations, simulating direct oxidation. Even when the available combinations of algorithms allowed the electronic wave functions to converge in these cases, the electronic structure was not of the required oxidation state of the Mn centers. Rather, the converged state was of a lower Mn oxidation state with oxidation occurring in the ligands.

As shown in Table 1, the direct oxidation of **A** resulted in frequency changes of 46−196 cm^{-1} in the symmetric mode (uniformly negative) and up to 57 cm^{-1} in the asymmetric mode. Oxidation with deprotonation generally gave substantially smaller changes in both the symmetric and asymmetric modes, though some calculated changes in the frequencies would be easily observable in difference spectra.

For the cases that could be converged on direct oxidation of the dinuclear manganese complex **B**, much larger frequency changes were observed than for the corresponding oxidations with deprotonation (Table 2). Convergence of the wave functions for oxidation with deprotonation was straightforward for all methods up to the second oxidation. However, even with deprotonation **B** could only be oxidized up to the Mn(III)−Mn(III) state, irrespective of which ligands were further deprotonated. Exploratory complete active space self-consistent field (CASSCF) calculations indicate that static correlation between d electrons is negligible in this system.

dx.doi.org/10.1021/jp500362q | J. Phys. Chem. B 2014, 118, 3553−3558

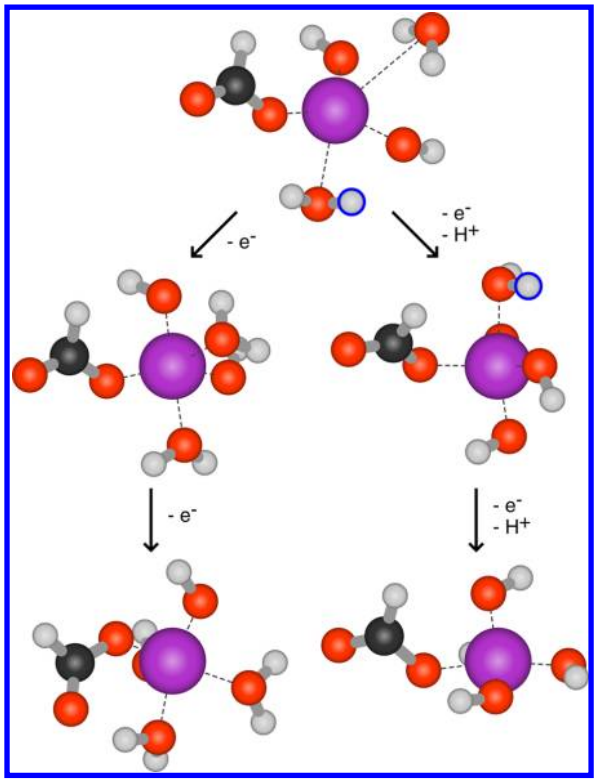

Figure 2. Geometries of cluster **A**, $Mn(H_2O)_2(OH)_2(HCOO)$. Geometries shown for Mn(II) (top), Mn(III) (middle), and Mn(IV) (bottom) complexes, with (right) and without (left) coupled deprotonation. Protons to be removed are highlighted with a blue border.

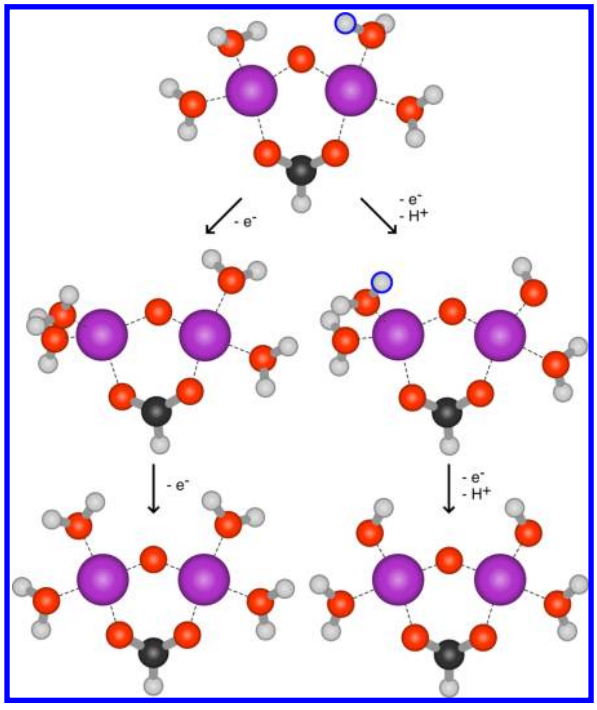

Figure 3. Geometries of cluster **B**, $Mn_2O(H_2O)_4(HCOO)$. Geometries shown for Mn(II)−Mn(II) (top), Mn(III)−Mn(II) (middle), and Mn(III)−Mn(III) (bottom) complexes, with (right) and without (left) coupled deprotonation. Protons to be removed are highlighted with a blue border.

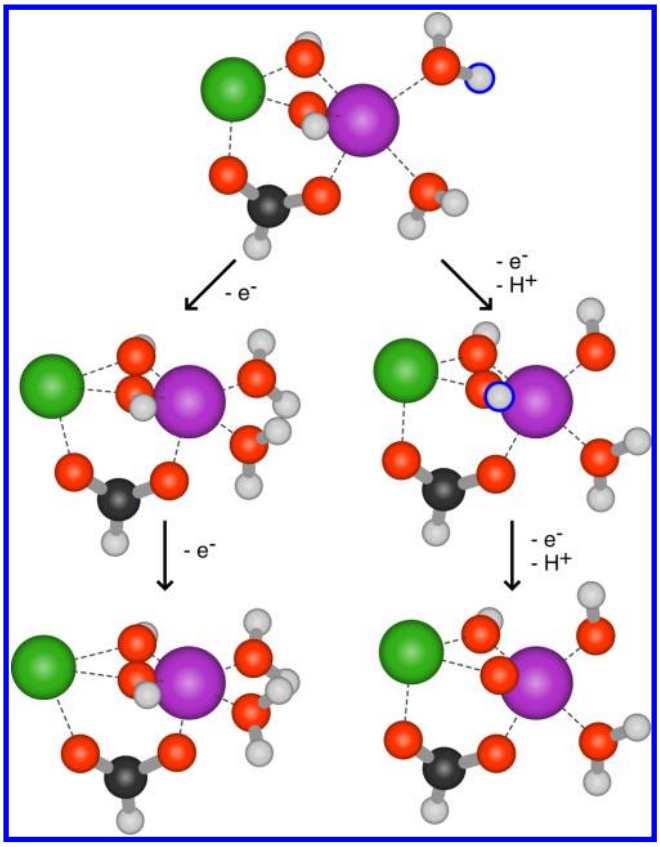

Figure 4. Geometries of cluster **C**, $MnCa(H_2O)_2(OH)_2(HCOO)$. Geometries shown for Mn(II) (top), Mn(III) (middle), and Mn(IV) (bottom) complexes, with (right) and without (left) coupled deprotonation. Protons to be removed are highlighted with a blue border.

Table 1. Frequency Shifts of the Carboxylate Stretching Modes of A upon Oxidation (cm^{-1})

		with deprotonation		direct oxidation	
method	transition	symm	asymm	symm	asymm
HF	II/III	+7	−13	−71	+54
	III/IV	−43	+11	−46	−57
MP2	II/III	+12	−13	−78	+20
	III/IV	−7	+8		
M06L	II/III	+13	−21	−75	+24
	III/IV	−34	+2	−196	−10
CCSD[a]	II/III	+5	−9	−76	+37
	III/IV	−45	+1		

[a]CCSD/6-31G(d,p).

Table 2. Frequency Shifts of the Carboxylate Stretching Modes of B upon Oxidation (cm^{-1})

		with deprotonation		direct oxidation	
method	transition	symm	asymm	symm	asymm
HF	II,II/II,III	−7	+4	−64	+23
	II,III/III,III	+21	−15	+62	−108
MP2	II,II/II,III	+9	+10		
	II,III/III,III	+13	−18		
M06L	II,II/II,III	+6	−22	−56	−30
	II,III/III,III	+3	+1	+12	−110

dx.doi.org/10.1021/jp500362q | J. Phys. Chem. B 2014, 118, 3553−3558

Table 3. Frequency Shifts of the Carboxylate Stretching Modes of C Upon Oxidation (cm^{-1})

		with deprotonation		direct oxidation	
method	transition	symm	asymm	symm	asymm
HF	II/III	+8	−3	0	−23
	III/IV	−4	−11	−277	+72
MP2	II/III	−4	−15	−13	−47
	III/IV	+11	+1		
M06L	II/III	−6	−10	−35	−22
	III/IV	−5	−13	−286	+57
CCSD[a]	II/III	−7	−11	−68	−36
	III/IV	+4	−11		

[a]CCSD/6-31G(d,p).

Structure **C** is a model of carboxylate bridging between Mn and Ca ions. The results given in Table 3 once more indicate that oxidation with deprotonation generally caused much smaller frequency changes than direct oxidation, with no method giving an oxidation with deprotonation frequency change greater than 15 cm^{-1}. In the Mn(III)/Mn(IV) transition, oxidation with deprotonation of a water ligand led to ligand oxidation and some convergence difficulties, whereas oxidation with deprotonation of a hydroxo bridge led to manganese oxidation, with minimal carboxylate frequency changes.

As can be seen from the frequencies listed in the Supporting Information, there was not a substantial difference between the changes to the vibrational frequency calculated using the Mn and Ca SDD basis sets (Tables 1−3) and those calculated using the 6-31G(d,p) basis set throughout. In particular, the frequencies calculated with the 6-31G(d,p) basis set conformed the pattern of large changes (up to 250 cm^{-1}) for direct oxidation and substantially smaller changes (at most 12 cm^{-1} for clusters **B** and **C**, generally smaller) for oxidation with deprotonation. The results thus do not appear to be particularly sensitive to the basis sets used for the metal centers.

Representative redox potentials are shown in Table 4. This table demonstrates a dramatic redox potential balancing effect

Table 4. Redox Potentials (eV) of All Three Clusters with and without Deprotonation, Calculated Using the M06L Method

	first oxidation[a]		second oxidation[b]	
cluster	deprotonated	direct ox.	deprotonated	direct ox.
A	2.87	1.81	2.95	7.71
B	2.61	9.32	3.00	15.13
C	3.25	10.44	3.96	16.18

[a]II/III for **A** and **C**, II,II/II,III for **B**. [b]III/IV for **A** and **C**, II,III/III,III for **B**.

when the clusters were oxidized with deprotonation. The Mn(II)/Mn(III) and Mn(III)/Mn(IV) redox couples were within ∼1 eV of each other with deprotonation, whereas a much larger difference was observed in the direct oxidation case. Deprotonation also significantly reduced the redox potentials of **B** and **C**, though the redox potential of the Mn(II)/Mn(III) couple in **A** increased by about 1 eV for the coupled deprotonation.

DISCUSSION

This work shows that the deprotonation of water/hydroxo ligands has a significant damping effect on oxidation-related frequency changes in carboxylate coligand stretching vibrations. Direct oxidation causes frequency changes much larger than the "oxidation with deprotonation" case in which ligand protons are removed simultaneously with the oxidation. Bridging carboxylate ligands, in particular, the Mn−Ca bridged **C**, have small enough frequency shifts on oxidation with deprotonation to potentially evade experimental detection (<∼10 cm^{-1}). This work, together with the available experimental evidence,[1,7] supports this as a general feature of Mn-carboxylate-water complexes.

Deprotonation of a hydroxo group was explored in this work (with a Mn−Ca bridging motif, **C**). The deprotonatable hydroxo bridge in **C** somewhat resembles the O5 center in the 1.9 Å crystal structure,[17,18] which might be mechanistically relevant for substrate water location.[33]

Water deprotonation is known to reduce the redox potential of multicentered manganese complexes,[2,3] which is consistent with the findings in this study. Though the redox potentials calculated in this work are higher than those that must operate in biological systems such as PS II,[4] it is important to note that the present calculations are for complexes in the gas phase without corrections for environmental dielectric, conformational and vibrational effects.[34,35] However, the computational results clearly highlight the importance of ligand deprotonation in maintaining near-constant redox potentials over multiple oxidation states in these manganese complexes.

Substantial difficulties were encountered in attempting to calculate electronic wave functions corresponding to many of the direct oxidation scenarios. No such difficulties were encountered when a ligand was deprotonated simultaneously. This suggests that the deprotonation of a H_nO ligand has a compensatory effect on the electronic and chemical changes wrought by oxidation of the manganese ion, consistent with minimal changes to the carboxylate ligand stretching frequencies.

The calculated frequency changes with deprotonation for cluster **C** were smaller and more consistent than those calculated for clusters **A** and **B**. It is notable that the conformation of the ligands of **C** barely changed when this cluster was oxidized with deprotonation. Cluster **A**, and to a lesser extent cluster **B**, underwent a greater degree of ligand position modification on oxidation than cluster **C** (Figures 2−4). One may speculate that at least some of the slightly larger frequency change for clusters **A** and **B** on oxidation with deprotonation can be attributed to ligand rearrangement in these unconstrained, gas phase models. If one considers these gas phase models to be representative of a small part of a larger, condensed system, then one would expect that ligand rearrangement would be somewhat restricted by the surrounding environment, which, in biological systems, would include the covalent tethering of the carboxylates to polypeptide backbones. If so, this would further reduce the observable frequency change for the carboxylate stretches under the influence of coupled oxidation and ligand deprotonation.

This study was motivated by FTIR spectroscopy of the WOC of PS II. It has been suggested that electronic charges in the WOC are inherently delocalized over the Mn centers,[36−41] which is not explicitly examinable though our model clusters beyond two metal centers. It is not then immediately obvious

dx.doi.org/10.1021/jp500362q | J. Phys. Chem. B 2014, 118, 3553−3558

how the current results relate to the FTIR spectroscopy of PS II, though we do note that sophisticated calculations that do not resort to density functional theory (which has a known propensity to overestimate delocalization[42]) indicate that the delocalization may be at the dimer level.[41] If we do take our results to be applicable to the WOC of PS II, then the observation that no proton is released from the WOC in the S_2/S_1 transition[43] would suggest that a frequency difference in the carboxylate modes should be most readily observed there.

CONCLUSION

In summary, our calculations show the following:

1. Oxidative changes of carboxylate stretch vibrational frequencies are significantly smaller when accompanied by deprotonation of water/hydroxo coligands.
2. The dampening of changes in the frequencies of ligated carboxylate vibrations depends on the coordination mode of the carboxylate. It appears to be more effective for bridging carboxylates than unidentate carboxylates in our gas phase model clusters. This suggests that deprotonation of adjacent ligands (waters, hydroxides) dampens frequency changes in at least bridging carboxylate ligands, to the point where they cannot be reliably detected at the level of resolution used in conventional FTIR difference spectroscopy experiments.
3. Deprotonation of water and/or hydroxo ligands maintains the redox potential of manganese complexes, allowing for successive oxidations by a near constant potential.
4. On oxidation, deprotonation of water and/or hydroxo ligands yields a thermodynamically more stable product (in the gas phase) in most cases.
5. For certain states of the tested hydroxo-bridged metal dimer cluster, deprotonation of a hydroxo bridge was required to achieve metal-center oxidation in the model cluster.

At present, the locations of Mn redox changes in the WOC catalytic center during turnover, and even the mean oxidation levels of the Mn cluster itself, are matters of contention.[44] This work, combined with available FTIR data, suggests that the availability of deprotonatable ligands may be an important factor to be considered when proposals for changes in manganese oxidation states throughout the WOC catalytic cycle are assessed.

ASSOCIATED CONTENT

Supporting Information

The calculated carboxylate vibrational frequencies for each cluster in the considered oxidation and protonation states are presented in a Supporting Information document. Results from calculations using both the 6-31G(d,p) and mixed 6-31G(d,p)/SDD basis sets are included. This material is available free of charge via the Internet at http://pubs.acs.org/.

AUTHOR INFORMATION

Corresponding Authors

*R. Stranger: e-mail, Rob.Stranger@anu.edu.au.
*R. J. Pace: e-mail, Ron.Pace@anu.edu.au.
*E. Krausz: e-mail, krausz@rsc.anu.edu.au.
*T. J. Fankcombe: e-mail, tjf@rsc.anu.edu.au.

Notes

The authors declare no competing financial interest.

ACKNOWLEDGMENTS

This work was supported by the NCI National Facility at the ANU.

REFERENCES

(1) Eilers, G.; Zettersten, C.; Nyholm, L.; Hammarström, L.; Lomoth, R. Ligand Exchange Upon Oxidation of a Dinuclear Mn Complex—Detection of Structural Changes by FT-IR Spectroscopy and ESI-MS. *Dalton Trans.* **2005**, 1033−1041.
(2) Thorp, H. H.; Sarneski, J. E.; Brudvig, G. W.; Crabtree, R. H. Proton-Coupled Electron Transfer in Manganese Complex $[(bpy)_2Mn(O)_2Mn(bpy)_2]^{3+}$. *J. Am. Chem. Soc.* **1989**, *111*, 9249−9250.
(3) Baldwin, M. J.; Pecoraro, V. L. Energetics of Proton-Coupled Electron Transfer in High-Valent $Mn_2(\mu\text{-}O)_2$ Systems: Models for Water Oxidation by the Oxygen-Evolving Complex of Photosystem II. *J. Am. Chem. Soc.* **1996**, *118*, 11325−11326.
(4) Pace, R. J.; Stranger, R.; Petrie, S. Why Nature Chose Mn for the Water Oxidase in Photosystem II. *Dalton Trans.* **2012**, *41*, 7179−7189.
(5) Elizarova, G. L.; Zhidomirov, G. M.; Parmon, V. N. Hydroxides of Transition Metals as Artificial Catalysts for Oxidation of Water to Dioxygen. *Catal. Today* **2000**, *58*, 71−88.
(6) Wang, T.; Brudvig, G. W.; Batista, V. S. Study of Proton Coupled Electron Transfer in a Biomimetic Dimanganese Water Oxidation Catalyst with Terminal Water Ligands. *J. Chem. Theory Comput.* **2010**, *6*, 2395−2401.
(7) Berggren, G.; Anderlund, M. F.; Styring, S.; Thapper, A. FTIR Study of Manganese Dimers with Carboxylate Donors as Model Complexes for the Water Oxidation Complex in Photosystem II. *Inorg. chem.* **2012**, *51*, 2332−2337.
(8) Wydrzynski, T. J.; Satoh, K. *Photosystem II: The Light Driven Water: Plastoquinone Oxidoreductase*; Photosynthesis Research; Springer: Netherlands, 2006; Vol. *87*; pp 331−335.
(9) Cox, N.; Messinger, J. Reflections on Substrate Water and Dioxygen Formation. *Biochim. Biophys. Acta* **2013**, *1827*, 1020−1030.
(10) Messinger, J.; Noguchi, T.; Yano, J. In *Molecular Solar Fuels*; Wydrzynski, T. J., Hillier, W., Eds.; RSC Publishing: Cambridge, U.K., 2012; Chapter 7, pp 163−207.
(11) Debus, R. J. The Manganese and Calcium Ions of Photosynthetic Oxygen Evolution. *Biochim. Biophys. Acta* **1992**, *1102*, 269−352.
(12) Debus, R. J. Protein Ligation of the Photosynthetic Oxygen-Evolving Center. *Coord. Chem. Rev.* **2008**, *252*, 244−258.
(13) Zouni, A.; Witt, H.-T.; Kern, J.; Fromme, P.; Krauss, N.; Saenger, W.; Orth, P. Crystal Structure of Photosystem II from Synechococcus Elongatus at 3.8 Å Resolution. *Nature* **2001**, *409*, 739−743.
(14) Kamiya, N.; Shen, J.-R. Crystal Structure of Oxygen-Evolving Photosystem II from Thermosynechococcus Vulcanus at 3.7-Å Resolution. *Proc. Natl. Acad. Sci.* **2003**, *100*, 98−103.
(15) Loll, B.; Kern, J.; Saenger, W.; Zouni, A.; Biesiadka, J. Towards Complete Cofactor Arrangement in the 3.0 Å Resolution Structure of Photosystem II. *Nature* **2005**, *438*, 1040−1044.
(16) Guskov, A.; Kern, J.; Gabdulkhakov, A.; Broser, M.; Zouni, A.; Saenger, W. Cyanobacterial Photosystem II at 2.9-Å Resolution and the Role of Quinones, Lipids, Channels and Chloride. *Nat. Struct. Mol. Biol.* **2009**, *16*, 334−342.
(17) Kawakami, K.; Umena, Y.; Kamiya, N.; Shen, J.-R. Structure of the Catalytic, Inorganic Core of Oxygen-Evolving Photosystem II at 1.9 Å Resolution. *J. Photochem. Photobiol. B: Biol.* **2011**, *104*, 9−18.
(18) Umena, Y.; Kawakami, K.; Shen, J.-R.; Kamiya, N. Crystal Structure of Oxygen-Evolving Photosystem II at a Resolution of 1.9 Å. *Nature* **2011**, *473*, 55−61.
(19) Dau, H.; Haumann, M. The Manganese Complex of Photosystem II in its Reaction Cycle—Basic Framework and Possible Realization at the Atomic Level. *Coord. Chem. Rev.* **2008**, *252*, 273−295.

(20) Service, R. J.; Hillier, W.; Debus, R. J. Evidence from FTIR Difference Spectroscopy of an Extensive Network of Hydrogen Bonds near the Oxygen-Evolving Mn_4Ca Cluster of Photosystem II Involving D1-Glu65, D2-Glu312, and D1-Glu329. *Biochemistry.* **2010**, *49*, 6655−6669.
(21) Suzuki, H.; Yu, J.; Kobayashi, T.; Nakanishi, H.; Nixon, P. J.; Noguchi, T. Functional Roles of D2-Lys317 and the Interacting Chloride Ion in the Water Oxidation Reaction of Photosystem II As Revealed by Fourier Transform Infrared Analysis. *Biochemistry* **2013**, *52*, 4748−4757.
(22) Pokhrel, R.; Service, R. J.; Debus, R. J.; Brudvig, G. W. Mutation of Lysine 317 in the D2 Subunit of Photosystem II Alters Chloride Binding and Proton Transport. *Biochemistry* **2013**, *52*, 4758−4773.
(23) Polander, B. C.; Barry, B. A. Detection of an Intermediary, Protonated Water Cluster in Photosynthetic Oxygen Evolution. *Proc. Natl. Acad. Sci.* **2013**, *110*, 10634−10639.
(24) Vassiliev, S.; Zaraiskaya, T.; Bruce, D. Molecular Dynamics Simulations Reveal High Permiability Oxygen Exit Channels Shared With Water Uptake Channels in Photosystem II. *Biochim. Biophys. Acta* **2013**, *1827*, 1148−1155.
(25) Kimura, Y.; Mizusawa, N.; Yamanari, T.; Ishi, A.; Ono, T.-A. Structural Changes of D1 C-terminal α-Carboxylate during S-state Cycling in Photosynthetic Oxygen Evolution. *J. Biol. Chem.* **2005**, *280*, 2078−2083.
(26) Chu, H.-A.; Hillier, W.; Debus, R. J. Evidence that the C-Terminus of the D1 Polypeptide of Photosystem II is Ligated to the Manganese Ion that Undergoes Oxidation During the S_1 to S_2 Transition: An Isotope-Edited FTIR Study. *Biochemistry* **2004**, *43*, 3152−3166.
(27) Service, R. J.; Yano, J.; McConnell, I.; Hwang, H. J.; Niks, D.; Hille, R.; Wydrzynski, T.; Burnap, R. L.; Hillier, W.; Debus, R. J. Participation of Glutamate-354 of the CP43 Polypeptide in the Ligation of Manganese and the Binding of Substrate Water in Photosystem II. *Biochemistry* **2011**, *50*, 63−81.
(28) Shimada, Y.; Suzuki, H.; Tsuchiya, T.; Tomo, T.; Noguchi, T.; Mimuro, M. Effect of a Single-Amino Acid Substitution of the 43 kDa Chlorophyll Protein on the Oxygen-Evolving Reaction of the Cyanobacterium Synechocystis sp. PCC 6803: Analysis of the Glu354Gln Mutation. *Biochemistry* **2009**, *48*, 6095−6103.
(29) Service, R. J.; Yano, J.; Dilbeck, P. L.; Burnap, R. L.; Hillier, W.; Debus, R. J. Participation of Glutamate-333 of the D1 Polypeptide in the Ligation of the Mn_4CaO_5 Cluster in Photosystem II. *Biochemistry* **2013**, *52*, 8452−8464.
(30) Strickler, M. A.; Walker, L. M.; Hillier, W.; Britt, R. D.; Debus, R. J. No Evidence from FTIR Difference Spectroscopy That Aspartate-342 of the D1 Polypeptide Ligates a Mn Ion That Undergoes Oxidation during the S_0 to S_1, S_1 to S_2, or S_2 to S_3 Transitions in Photosystem II. *Biochemistry* **2007**, *46*, 3151−3160.
(31) Pace, R. J.; Jin, L.; Stranger, R. What Spectroscopy Reveals Concerning the Mn Oxidation Levels in the Oxygen Evolving Complex of Photosystem II: X-Ray to Near Infra-Red. *Dalton Trans.* **2012**, *41*, 11145−11160.
(32) Frisch, M. J.; et al. *Gaussian 09*, Revision D.01; Gaussian Inc.: Wallingford, CT, 2009.
(33) Rapatskiy, L.; Cox, N.; Savitsky, A.; Ames, W. M.; Sander, J.; Nowaczyk, M. M.; Rögner, M.; Boussac, A.; Neese, F.; Messinger, J. Detection of the Water-Binding Sites of the Oxygen-Evolving Complex of Photosystem II Using W-Band ^{17}O Electron−Electron Double Resonance-Detected NMR Spectroscopy. *J. Am. Chem. Soc.* **2012**, *134*, 16619−16634.
(34) Formaneck, M. S.; Li, G.; Zhang, X.; Cui, Q. Calculating Accurate Redox Potentials in Enzymes with a Combined QM/MM Free Energy Perturbation Approach. *J. Theor. Comput. Chem.* **2002**, *1*, 53−67.
(35) Mahboob, A.; Vassiliev, S.; Poddutoori, P. K.; van der Est, A.; Bruce, D. Factors Controlling the Redox Potential of $ZnCe_6$ in an Engineered Bacterioferritin Photochemical 'Reaction Centre'. *PLOS One* **2013**, *8*, e68421.
(36) Sproviero, E. M.; Gascón, J. A.; McEvoy, J. P.; Brudvig, G. W.; Batista, V. S. Quantum Mechanics/Molecular Mechanics Study of the Catalytic Cycle of Water Splitting in Photosystem II. *J. Am. Chem. Soc.* **2008**, *130*, 3428−3442.
(37) Sproviero, E. M.; Gascón, J. A.; McEvoy, J. P.; Brudvig, G. W.; Batista, V. S. Characterization of Synthetic Oxomanganese Complexes and the Inorganic Core of the O_2-Evolving Complex in Photosystem II: Evaluation of the DFT/B3LYP Level of Theory. *J. Inorg. Biochem.* **2006**, *100*, 786−800.
(38) McGrady, J. E.; Stranger, R. Redox-Induced Changes in the Geometry and Electronic Structure of Di-μ-oxo-Bridged Manganese Dimers. *J. Am. Chem. Soc.* **1997**, *119*, 8512−8522.
(39) Glatzel, P.; Bergmann, U.; Yano, J.; Visser, H.; Robblee, J. H.; Gu, W.; de Groot, F. M. F.; Christou, G.; Pecoraro, V. L.; Cramer, S. P.; Yachandra, V. K. The Electronic Structure of Mn in Oxides, Coordination Complexes, and the Oxygen-Evolving Complex of Photosystem II Studied by Resonant Inelastic X-ray Scattering. *J. Am. Chem. Soc.* **2004**, *126*, 9946−9959.
(40) Glatzel, P.; Schroeder, H.; Pushkar, Y.; Boron, T., III; Mukherjee, S.; Christou, G.; Pecoraro, V. L.; Messinger, J.; Yachandra, V. K.; Bergmann, U.; Yano, J. Electronic Structural Changes of Mn in the Oxygen-Evolving Complex of Photosystem II during the Catalytic Cycle. *Inorg. Chem.* **2013**, *52*, 5642−5644.
(41) Kurashige, Y.; Chan, G. K.-L.; Yanai, T. Entangled Quantum Electronic Wavefunctions of the Mn_4CaO_5 Cluster in Photosystem II. *Nat. Chem.* **2013**, *5*, 660−666.
(42) Cohen, A. J.; Mori-Sánchez, P.; Yang, W. Insights into Current Limitations of Density Functional Theory. *Science* **2008**, *321*, 792−794.
(43) Suzuki, H.; Sugiura, M.; Noguchi, T. Monitoring Proton Release During Photosynthetic Water Oxidation in Photosystem II by Means of Isotope-Edited Infrared Spectroscopy. *J. Am. Chem. Soc.* **2009**, *131*, 7849−7857.
(44) Gatt, P.; Stranger, R.; Pace, R. J. Application of Computational Chemistry to Understanding the Structure and Mechanism of the Mn Catalytic Site in Photosystem II — A Review. *J. Photochem. Photobiol. B: Biol.* **2011**, *104*, 80−93.